

Local Lattice Structure Study of the Octahedral $(\text{CrO}_6)^{9-}$ Clusters for Cr^{3+} Ion Doping in a Variety of Oxide Crystals by Simulating the Corresponding EPR and Optical Spectra

Kuang Xiao-Yu,^{*,†,‡} Mao Ai-Jie,[†] and Wang Hui[†]

Institute of Atomic and Molecular Physics, Sichuan University, Chengdu 610065, China, and International Centre for Materials Physics, Academia Sinica, Shenyang 110016, China

Received: August 4, 2007; In Final Form: October 18, 2007

On the basis of the 120×120 complete energy matrix, the local lattice structures of the octahedral $(\text{CrO}_6)^{9-}$ clusters for Cr^{3+} ions doping in a variety of oxide crystals with D_{3d} or C_{3v} site symmetry have been studied by employing two distorted parameters, respectively. By simulating the calculated EPR and optical spectra data to the experimental results, the local lattice structure parameters are determined unambiguously. It is shown, by means of a series of calculations, that although the local lattice structures around the M ($M = \text{Al}^{3+}, \text{Ga}^{3+}, \text{Li}^+, \text{Sc}^{3+}$, etc.) ions in host crystals are obviously different, the local lattice structures of the octahedral $(\text{CrO}_6)^{9-}$ clusters in a variety of oxide crystals doped with Cr^{3+} ions are similar and fluctuant in the vicinity of that of the Cr_2O_3 . This may be ascribed to the fact that there is the similarly octahedral $(\text{CrO}_6)^{9-}$ clusters in a variety of oxide crystals doped with Cr^{3+} and the Cr_2O_3 crystal. Our viewpoint is consistent with that of Gaudry et al. [Phys. Rev. B 2003, 67, 094108].

I. Introduction

To study the inter-relation between the molecular structure and the electronic structure of the transition metal ions in the complex molecules by employing an EPR mechanism is an interesting and important problem. Up to now, four theoretical methods have been employed to investigate the zero-field splitting of the transition metal ion doping in crystals. The first is ab initio calculations,^{1–4} the ZFS is generally reckoned using an electrostatic model of the crystal field, together with one or more of the splitting mechanisms. The second is the empirical superposition model by analyzing the spin Hamiltonian.^{5–6} The third and fourth methods are both developed on the basis of the empirical superposition model: one of them is the high-order perturbation^{7–8} and the other is the complete energy matrix.^{9–10} Especially, the complete energy matrices have recently been extensively applied to deal with the systems doped with transition metal ions. In this paper, we will study the total properties of the octahedral $(\text{CrO}_6)^{9-}$ clusters for Cr^{3+} ion doping in a variety of oxide crystals with D_{3d} or C_{3v} site symmetry by employing the complete energy matrix.

Oxide crystals exist in any or every place of our surroundings and play an important role in our diet, environment, health, work, and so on. So there is a continuing interest in the study of the relational properties of oxide crystals from both the experiment and theory. Thus, it has been found that transition metals (Fe, Mn, and Cr) doped in oxide crystals have been shown to improve the relational properties of oxide crystals (such as domain structure, electro-optical coefficients, light absorption, refractive indices, etc.). So the study of the electric and magnetic structures of Cr^{3+} complexes is an interesting and important problem. It is well known that, as for a d^3 configuration ion in a trigonal ligand field, only the EPR and optical spectra

TABLE 1: Host Structures and the Local Lattice Structures of the $(\text{CrO}_6)^{9-}$ Clusters in the Oxide Crystals with D_{3d} Symmetry Doped with Cr^{3+} Ions, Dq in Units of cm^{-1}

compound	T (K)	Dq	$R_0 (\text{\AA})$	$\theta_0 (\text{deg})$	$R (\text{\AA})$	$\theta (\text{deg})$	refs
ZnAl ₂ O ₄	300	1876	1.915	49.94	1.956	52.528	20
MgAl ₂ O ₄	300	1850	1.928	50.66	1.961	52.570	20
ZnGa ₂ O ₄	77	1840	1.988	50.66	1.970	53.510	20
Y ₃ Ga ₅ O ₁₂	77	1650	1.995	51.7	2.015	53.844	21
Y ₃ Al ₅ O ₁₂	77	1640	1.937	52.5	2.019	54.750	21
Be ₃ Al ₂ Si ₆ O ₁₈	300	1620	1.906		2.020	57.344	22
KAl(MoO ₄)	300	1497	2.000	53.64	2.051	53.601	23
RbSc(MoO ₄)	300	1445	2.007	48.97	2.062	55.909	24–25
KSc(MoO ₄)	300	1435	2.010	51.37	2.066	55.826	24–25
RbIn(MoO ₄)	300	1400	2.020	48.99	2.074	56.030	23

can get satisfactory explanation simultaneously, the related properties of d^3 complexes can be determined by employing two distorted parameters. In this paper, local lattice structures of the trigonal octahedral $(\text{CrO}_6)^{9-}$ clusters for Cr^{3+} ions doping in a variety of oxide crystals with D_{3d} or C_{3v} site symmetry have been investigated by employing two distorted parameters, respectively. The calculated results show that although the local lattice structures around the M ($M = \text{Al}^{3+}, \text{Ga}^{3+}, \text{Li}^+, \text{Sc}^{3+}$ etc.) ions in host crystals are obviously different, the local lattice structures of the octahedral $(\text{CrO}_6)^{9-}$ clusters in a variety of oxide crystals doped with Cr^{3+} ions are similar and fluctuant in the vicinity of that of the Cr_2O_3 . The sensitive relation between the crystal field strength Dq and the average values \bar{R} of Cr–O bond length will be analyzed further.

II. Theoretical Method

By employing the $|L, M_l, S, M_s\rangle$ basic function of a d^3 configuration ion at trigonal symmetry site, we have constructed the complete energy matrix of the Hamiltonian^{11–12}

$$\hat{H} = \hat{H}_{ee} + \hat{H}_{LF} + \hat{H}_{SO} + \hat{H}_{ZE} \\ = \sum_{i,j} e^2/r_{i,j} + \sum_i V_i + \xi \sum_i l_i \cdot s_i + \mu_\beta \sum_i (k \vec{l}_i + g_e \vec{s}_i) \cdot \vec{H} \quad (1)$$

* Corresponding author. Mailing address: Institute of Atomic and Molecular Physics, Sichuan University, Chengdu 610065, China. E-mail address: scu_kxy@163.com.

† Sichuan University.

‡ Academia Sinica.

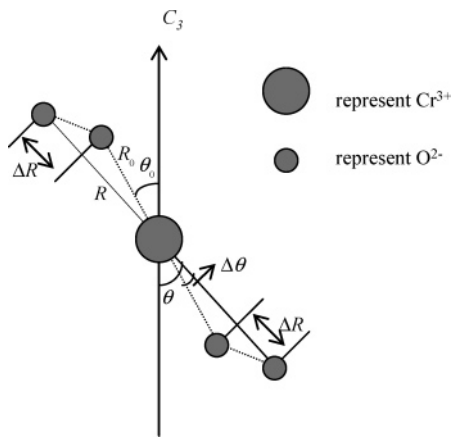


Figure 1. Local structure of octahedral Cr^{3+} centers in oxide crystals with D_{3d} symmetry. R_0 and θ_0 are the structure parameters of host crystals; R and θ are the impurity structure parameters. ΔR and $\Delta\theta$ represent the structure distortion.

TABLE 2: Racah Parameters B and C , the Spin–Orbit Coupling Coefficient ζ and the Orbit Reduction Factor k for Cr^{3+} Ion Doped in a Variety of Oxide Crystals with D_{3d} or C_{3v} Symmetry, with All Units in cm^{-1} Except for the Orbit Reduction Factor k

compound	B	C	ζ	k	refs
ZnAl ₂ O ₄	700	3200	250	0.74	26
MgAl ₂ O ₄	700	3200	250	0.58	26
ZnGa ₂ O ₄	670	3230	250	0.76	27
Y ₃ Al ₅ O ₁₂	650	3250	234	0.70	28
Y ₃ Ga ₅ O ₁₂	570	3400	230	0.74	28
Be ₃ Al ₂ Si ₆ O ₁₈ ^a	780	2960	225	0.70	29
KAl(MoO ₄)	648	2917	227	0.66	30
RbSc(MoO ₄)	681	2902	229	0.82	30
KSc(MoO ₄)	681	2902	229	0.82	30
RbIn(MoO ₄)	681	2902	229	0.81	30–31
Al ₂ O ₃	650	3120	170	0.68	32–33
LiNbO ₃	558	3204	195	0.82	34
LiTaO ₃	667	3012	231	0.75	35
LiIO ₃	668	2672	224	0.82	36–37

^a Be₃Al₂Si₆O₁₈; the Trees correction $\alpha = 70 \text{ cm}^{-1}$ is also employing in the calculation.

where \hat{H}_{ee} , \hat{H}_{LF} , \hat{H}_{SO} , and \hat{H}_{ZE} are, respectively, the electron–electron repulsion interaction, the ligand-field interaction, the spin–orbit coupling interaction, and the Zeeman interaction. ζ is the spin–orbit coupling coefficient, k is the orbit reduction factor and V_i is the ligand-field potential

$$V_i = \gamma_{00}Z_{00} + \gamma_{20}r_i^2Z_{20}(\theta_i, \varphi_i) + \gamma_{40}r_i^4Z_{40}(\theta_i, \varphi_i) + \\ \gamma_{43}^cr_i^4Z_{43}^c(\theta_i, \varphi_i) + \gamma_{43}^sr_i^4Z_{43}^s(\theta_i, \varphi_i) \quad (2)$$

r_i , θ_i , and φ_i are the coordinates of the i th electron. According to the Hamiltonian (1), the 120×120 energy matrix for a d^3 configuration ion has been constructed. The matrix elements are functions of the Racah parameters B and C , the spin–orbit coupling coefficient ζ , and the ligand-field parameters that are of the forms for Cr^{3+} ions doping in a variety of oxide crystals with trigonal symmetry⁶

$$B_{20} = \frac{1}{2} \sum_{\tau} G_2(\tau)(3 \cos^2 \theta_{\tau} - 1),$$

$$B_{40} = \frac{1}{8} \sum_{\tau} G_4(\tau)(35 \cos^4 \theta_{\tau} - 30 \cos^2 \theta_{\tau} + 3),$$

TABLE 3: Comparison of Optical Spectra between the Theoretical and Experimental Values for Cr^{3+} Ions Doped in Oxide Crystals with D_{3d} Symmetry, where $A_4 = 36.35 \text{ a.u.}$ at Room Temperature and $A_4 = 36.53 \text{ a.u.}$ at Low Temperature (77 K), Respectively, with All Units in cm^{-1}

transitions	T (K)	2E	2T_1	4T_2	2T_2	4T_1
		$^4A_2 \rightarrow$	2E	2T_1	4T_2	2T_2
ZnAl ₂ O ₄	300	14556 15837	15098 20244	18727 23340	21573 26846	26025
Expt ²⁶		14570 14579		18756 23974		25832
MgAl ₂ O ₄	300	14561	15106 15824	18501 19973	21555 23273	25757 26574
Expt ²⁶		14660 14653	14812 15069	18500 15228	22100 24100	25800
ZnGa ₂ O ₄	77	14613	15134 15494	18427 19186	21778 22639	25308 25749
Expt ²⁷		14549 14589		18400 15108		23500 25000
Y ₃ Ga ₅ O ₁₂	77	14463	14879 15108	16519 17029	21463 21995	22451 22707
Expt ^{28,38–39}		14472 14450	14793	16260 16300	19305 16500	22727 22730
Y ₃ Al ₅ O ₁₂	77	14555	15077 15231	16425 16732	21610 21962	22915 23138
Expt ^{28,40}		14544 14564	15210 15425	16400 16700		23200
Be ₃ Al ₂ Si ₆ O ₁₈	300	14762	15322 15951	15719 16788	21537 23243	23177 24576
Expt ²⁹		14624 14686	15140	15860 16750	21037 24000	23000
KAl(MoO ₄)	300	13436	13970 14288	14992 15619	19756 20507	21292 21772
Expt ³⁰		13436	13969	14972		21266
RbSc(MoO ₄)	300	13585	14059 14394	14460 14978	20153 20817	21185 21782
KSc(MoO ₄)	300	13589	14070 14381	14340 14823	20135 20755	21031 21589
RbIn(MoO ₄)	300	13559	14024 14394	14011 14570	20052 20777	20682 21359
Expt ³¹		13560	14395	14024		20053

$$B_{43}^c = \frac{\sqrt{35}}{4} \sum_{\tau} G_4(\tau) \cos \theta_{\tau} \sin^3 \theta_{\tau} \cos 3\phi_{\tau},$$

$$B_{43}^s = i \frac{\sqrt{35}}{4} \sum_{\tau} G_4(\tau) \cos \theta_{\tau} \sin^3 \theta_{\tau} \sin 3\phi_{\tau} \quad (3)$$

where

$$G_2(\tau) = -q_{\tau}eG^2(\tau), \quad G_4(\tau) = -q_{\tau}eG^4(\tau)$$

$$G^k(\tau) = \int_0^{R_{\tau}} R_{3d}^{-2}(r) r^2 \frac{r^k}{R_{\tau}^{k+1}} dr + \int_{R_{\tau}}^{\infty} R_{3d}^{-2}(r) r^2 \frac{R_{\tau}^k}{r^{k+1}} dr \quad (4)$$

In explicitly, the Zeeman term can be expressed by parallel or perpendicular component to the C_3 axis as follows:

$$H_{ZE}(\parallel) = \mu_{\beta} \sum_i (kl_{iz} + g_e s_{iz}) H_z$$

$$H_{ZE}(\perp) = \mu_{\beta} \sum_i (kl_{ix} + g_e s_{ix}) H_x \quad (5)$$

By using eq 5, the 120×120 complete energy matrix including the parallel and perpendicular components of Zeeman term for a d^3 configuration ion in a trigonal ligand field has been constructed.

TABLE 4: Zero-Field Splitting Parameters D and g Factors for Cr³⁺ Ions Doped in a Variety of Oxide Crystals with D_{3d} Symmetry as a Function of the Two Parameters ΔR and $\Delta\theta$ by Employing $A_4 = 36.35$ a.u. at Room Temperature and $A_4 = 36.53$ a.u. at Low Temperature (77 K), Respectively, $2D$ in Units of cm⁻¹

compound	T (K)	ΔR (Å)	$\Delta\theta$ (deg)	$2D$	$g_{ }$	g_{\perp}	$\Delta g (=g_{ } - g_{\perp})$
ZnAl ₂ O ₄	300	0.041	2.588	1.8553	1.9808	1.9739	0.0069
expt ⁴¹				1.8556	1.9807	1.9774	0.0033
MgAl ₂ O ₄	300	0.033	1.910	1.834	1.9851	1.9797	0.0054
expt ²⁶				1.830	1.9850	1.9830	0.0020
ZnGa ₂ O ₄	77	-0.018	2.850	1.048	1.9773	1.9733	0.0040
expt ²⁷				1.048	1.9774	1.9761	0.0013
Y ₃ Ga ₅ O ₁₂	77	0.020	2.144	0.6971	1.9766	1.9736	0.0030
expt ⁴²				0.697	1.9767	1.9757	0.0010
Y ₃ Al ₅ O ₁₂	77	0.082	1.675	0.4502	1.9766	1.9748	0.0018
expt ⁴³				0.4502	1.9765	1.9765	0.0000
Be ₃ Al ₂ Si ₆ O ₁₈	300	0.114	2.608	-1.780	1.9719	1.9786	-0.0067
expt ^{29,33}				-1.780	1.9730	1.9700	0.0030
KAl(MoO ₄)	300	0.051	-0.039	0.9598	1.9780	1.9742	0.0038
expt ⁴⁴				0.9596	1.9781	1.9727	0.0054
RbSc(MoO ₄)	300	0.055	6.939	-0.9634	1.9649	1.9694	-0.0045
expt ⁴⁵				-0.9632	1.9646	1.9683	-0.0037
KSc(MoO ₄)	300	0.056	4.456	-0.9029	1.9647	1.9690	-0.0043
expt ⁴⁶				-0.9030	1.9645	1.9693	-0.0048
RbIn(MoO ₄)	300	0.054	7.040	-1.078	1.9639	1.9690	-0.0051
expt ⁴⁷				-1.080	1.9640	1.9680	-0.0040

TABLE 5: Original Structures of the Oxide Crystals with C_{3v} Symmetry

compound	R_{10} (Å)	R_{20} (Å)	θ_{10} (deg)	θ_{20} (deg)	refs
Al ₂ O ₃	1.857	1.966	63.1	47.7	18
LiNbO ₃	1.889	2.112	61.65	47.99	48
LiTaO ₃	1.91	2.072	60.18	49.44	49
LiIO ₃	2.11	2.13	52.90	52.05	50

TABLE 6: Comparison of Optical Spectra between Theoretical and Experimental Values for Cr³⁺ Ions Doped in Oxide Crystals with C_{3v} Symmetry by Employing $A_4 = 36.35$ a.u. at Room Temperature and $A_4 = 36.53$ a.u. at Low Temperature (77 K), Respectively, with All Units in cm⁻¹

transitions	$^4A_2 \rightarrow$	T (K)	2E	2T_1	4T_2	2T_2	4T_1
Al ₂ O ₃	77	14111	14570	18007	21441	24362	
			14856	18273	21984	25607	
expt ³²⁻³³		14418	15168	18000	20993	24400	
		14447	15190	18450	21068	25200	
					21357		
LiNbO ₃	77	13747	14009	15308	20394	20642	
			14384	15353	21136	21802	
expt ³⁴		13790	14340	15300	20200	21000	
LiTaO ₃	300	13897	14298	15288	20550	21591	
			14637	15456	21256	22594	
expt ³⁵		13902		15291		21807	
		13972					
LiIO ₃	77	12758	13211	14313	19055	20986	
			13635	14951	19878	21733	
expt ³⁶⁻³⁷				13800		20200	
				14400		20250	

The EPR spectra of Cr³⁺ ions in a trigonal ligand-field can be described by the spin Hamiltonian¹³

$$\hat{H}_S = g_{||}\mu_{\beta}H_zS_z + g_{\perp}\mu_{\beta}(H_xS_x + H_yS_y) + D[S_z^2 - (1/3)S(S+1)] \quad (6)$$

where, D is zero-field splitting parameter. From eq 1 the energy levels in the ground state 4A_2 without magnetic field are written as follows:

$$E(\pm 1/2) = -D$$

$$E(\pm 3/2) = D \quad (7)$$

TABLE 7: Zero-Field Splitting Parameters D and g Factors for Cr³⁺ Ions Doped in a Variety of Oxide Crystals with C_{3v} Symmetry as a Function of the Two Parameters ΔR and ΔX by Employing $A_4 = 36.35$ a.u. at Room Temperature and $A_4 = 36.53$ a.u. at Low Temperature (77 K), Respectively, $2D$ in Units of cm⁻¹

compd	T (K)	ΔR (Å)	ΔX (Å)	$2D$	$g_{ }$	g_{\perp}	$\Delta g (=g_{ } - g_{\perp})$
Al ₂ O ₃	77	0.0419	0.02878	-0.3831	1.9858	1.9869	-0.0011
expt ⁵¹⁻⁵²				-0.383	1.9840	1.9867	-0.0027
LiNbO ₃	77	0.040	0.03583	-0.7730	1.9719	1.9753	-0.0034
expt ⁵³				-0.773	1.9720		
LiTaO ₃	300	0.0472	0.04665	-0.888	1.9696	1.9728	-0.0032
expt ⁴²				-0.888	1.9720		
LiIO ₃	77	-0.054	0.0359	-1.2198	1.9647	1.9704	-0.0057
expt ⁵⁴				-1.2198	1.9650	1.9710	-0.0060

TABLE 8: Local Lattice Structures of the (CrO₆)⁹⁻ Clusters in a Oxide Crystals with C_{3v} Symmetry Doped with Cr³⁺ Ions, Dq in Units of cm^{-1a}

compd	T (K)	Dq	R_1 (Å)	R_2 (Å)	θ_1 (deg)	θ_2 (deg)	\bar{R} (Å)	$\bar{\theta}_a$ (deg)
Al ₂ O ₃	77	1800	1.8989	2.0079	62.530	47.610	1.9534	55.070
LiNbO ₃	77	1530	1.9290	2.1520	61.690	48.230	2.0405	54.960
LiTaO ₃	300	1529	1.9572	2.1192	60.520	49.890	2.0382	55.205
LiIO ₃	77	1430	2.054	2.0740	56.723	55.730	2.0640	56.227
Cr ₂ O ₃		1.967	2.018	61.4	49.0		1.9925	55.20

^a $A_4 = 36.35$ a.u. at Room Temperature and $A_4 = 36.53$ a.u. at Low Temperature (77 K) are employed in the calculation, in units of cm⁻¹.

The corresponding ground-state zero-field splitting ΔE can be expressed as a function of the parameter D

$$\Delta E = E(\pm 3/2) - E(\pm 1/2) = 2D \quad (8)$$

Based on eqs 3 and 8, the relationship between the local lattice structures of the octahedral Cr³⁺ centers in oxide crystals with D_{3d} or C_{3v} site symmetry and its EPR parameters as well as the optical spectra can be investigated by means of the complete energy matrix, respectively.

III. Theoretical Calculations

1. Local Lattice Structures of the Octahedral (CrO₆)⁹⁻ Clusters for Cr³⁺ ion Doping in Oxide Crystals with D_{3d} Site Symmetry. Be₃Al₂Si₆O₁₈, ZnAl₂O₄, MgAl₂O₄, Y₃Al₅O₁₂,

TABLE 9: EPR Parameters D and g Factors and the Energy Transition ${}^4A_2 \rightarrow {}^4T_2$ for Cr³⁺ Ions Doped in Oxide Crystals with C_{3v} Symmetry as a Function of the Two Parameters ΔR and ΔX by Employing $A_4 = 36.12$ a.u., $2D$ in Units of cm⁻¹

compound	ΔR (Å)	ΔX (Å)	$2D$	g_{\parallel}	g_{\perp}	${}^4A_2 \rightarrow {}^4T_2$ (cm ⁻¹)
Al ₂ O ₃ expt ^{32–33,51–52}	0.0374	0.02500	-0.3823	1.9858	1.9869	18003 18274
LiNbO ₃ expt ^{34,53}	0.0354	0.03200	-0.3830 -0.7729 -0.7730	1.9840 1.9719 1.9720	1.9867 1.9753	18000 18450 15308 15350 15300
LiTaO ₃ expt ^{35,42}	0.0445	0.0444	-0.887 -0.888	1.9696 1.9720	1.9728	15293 15459 15291
Li ₂ O ₃ expt ^{36–37,54}	-0.0584	0.03235	-1.2197 -1.2198	1.9647 1.9650	1.9704 1.9710	14304 14941 13800 14400

TABLE 10: EPR Parameters D and g Factors and the Energy Transition ${}^4A_2 \rightarrow {}^4T_2$ for Cr³⁺ Ions Doped in Oxide Crystals with D_{3d} Symmetry as a Function of the Two Parameters ΔR and $\Delta \theta$ by Employing $A_4 = 36.12$ a.u., $2D$ in Units of cm⁻¹

compound	ΔR (Å)	$\Delta \theta$ (deg)	$2D$	g_{\parallel}	g_{\perp}	${}^4A_2 \rightarrow {}^4T_2$ (cm ⁻¹)
ZnAl ₂ O ₄ expt ^{26,41}	0.038	2.581	1.8557 1.8556	1.9808 1.9807	1.9739 1.9774	18752 20269 18756
MgAl ₂ O ₄ expt ²⁶	0.0306	1.910	1.830 1.830	1.9851 1.9850	1.9797 1.9830	18499 19965 18500
ZnGa ₂ O ₄ expt ²⁷	-0.0218	2.847	1.048 1.048	1.9773 1.9774	1.9733 1.9761	18397 19153 18400
Y ₃ Ga ₅ O ₁₂ expt ^{28,38–39,42}	0.016	2.141	0.6973	1.9766	1.9736	16497 17005
Y ₃ Al ₅ O ₁₂ expt ^{28,40,43}	0.078	1.673	0.4504 0.4502	1.9766 1.9765	1.9748 1.9765	16403 16708 16400 16700
Be ₃ Al ₂ Si ₆ O ₁₈ expt ^{29,33}	0.111	2.615	-1.780 -1.780	1.9719 1.9730	1.9786 1.9700	15737 16805 15860 16750
KAl(MoO ₄) expt ^{30,44}	0.049	-0.040	0.9594 0.9596	1.9780 1.9781	1.9742 1.9727	14970 15595 14972
RbSc(MoO ₄) expt ⁴⁵	0.0527	6.941	-0.9634 -0.9632	1.9649 1.9646	1.9694 1.9683	14449 14967
KSc(MoO ₄) expt ⁴⁶	0.053	4.459	-0.9029 -0.9030	1.9647 1.9645	1.9690 1.9693	14354 14837
RbIn(MoO ₄) expt ^{31,47}	0.050	7.050	-1.083 -1.080	1.9639 1.9640	1.9690 1.9680	14022 14584 14024

KAl(MoO₄), ZnGa₂O₄, Y₃Ga₅O₁₂, RbSc(MoO₄), KSc(MoO₄), and RbIn(MoO₄) possess the D_{3d} point symmetry. When Cr³⁺ ions are doped in oxide crystals, the Cr³⁺ ion will replace the host ions (Al³⁺, Ga³⁺, Sc³⁺, or In³⁺). Cr³⁺ ion is surrounded by an oxygen octahedron which is distorted along the 3-fold axis. In the calculation, we choose the projection of one of the Cr–O bond in x – y plane along x axis. In this case, the B_{43}^s term is zero, and the ligand field parameters can be written as

$$B_{20} = 3G_2(\tau)(3 \cos^2 \theta - 1)$$

$$B_{40} = (3/4)G_4(\tau)(35 \cos^4 \theta - 30 \cos^2 \theta + 3)$$

$$B_{43}^c = (3\sqrt{35}/2)G_4(\tau) \cos \theta \sin^3 \theta \quad (9)$$

According to the van Vleck approximation for $G^k(\tau)$ integral,¹⁴ we may get the following relations:

$$G_2(\tau) = \frac{A_2}{R_\tau^3}, \quad G_4(\tau) = \frac{A_4}{R_\tau^5} \quad (10)$$

where $A_2 = -eq\langle r^2 \rangle$, $A_4 = -eq\langle r^4 \rangle$, and $A_2/A_4 = \langle r^2 \rangle/\langle r^4 \rangle$. The ratio of $\langle r^2 \rangle/\langle r^4 \rangle = 0.151227$ for Cr³⁺ may be obtained from the parametric radial wave function.¹⁵ The value of A_4 can be determined from the optical spectra and real local structure parameters of (CrO₆)⁹⁻ in different crystals. Herein, both the obviously different symmetry systems Cr₂O₃ and MgO:Cr³⁺ are

taken in our analysis. We derive $A_4=36.12$ a.u. for (CrO₆)⁹⁻ in MgO,^{16–17} Cr³⁺ and $A_4 = 36.35$ a.u. as well as $A_4 = 36.53$ a.u., respectively for the (CrO₆)⁹⁻ cluster in Cr₂O₃^{18–19} at room temperature and the low temperature (77 K). Also, the influences of the different A_4 value from different symmetry systems Cr₂O₃ and MgO:Cr³⁺ on the precision of the structure parameters are analyzed in the following. Correspondingly, the trigonal distortion can be described by means of two parameters ΔR and $\Delta \theta$, as plotted in Figure 1. Thus the impurity structural parameters R and θ can be expressed as

$$\begin{aligned} R &= R_0 + \Delta R \\ \theta &= \theta_0 + \Delta \theta \end{aligned} \quad (11)$$

where, R_0 and θ_0 denote the M–O (M = Al, Ga, Sc, In) bond length and the angle between M–O bond and the C_3 axis, respectively, and the values are listed in Table 1 (see refs 20–25). As for the Racah parameters B and C , the spin–orbit coupling coefficient ζ , and the orbit reduction factors k , the classical values are taken that approved by many researchers,^{26–37} which are listed in Table 2. As for the orbit reduction factor k , the slightly adjusted value from the formula $k \approx N^2 = (\sqrt{B/B_0} + \sqrt{C/C_0})/2$ or the classical value $k = 0.7^{28,32–33}$ has been made in order to obtain the precise calculations of the g factors (g_{\parallel}, g_{\perp}). By diagonalizing the complete energy matrix with trigonal symmetry and employing the above parameters, the optical and EPR spectra of the octahedral (CrO₆)⁹⁻ clusters for the Cr³⁺ ion doping in different oxide crystals with D_{3d} site symmetry are simulated by employing two distortion parameters ΔR and $\Delta \theta$, and the results are listed in Tables 1, 3, 4, and 10.

$$R_2 = R_{20} + \Delta R$$

TABLE 11: Comparison of Theoretical Structure Parameters (or Average Values) to Different A_4 Values for Cr^{3+} Ions Doped in Oxide Crystals with D_{3d} (or C_{3v}) Symmetry

compound	$R(\bar{R})$ (Å)		$\Delta R'$ (Å)	$\theta(\bar{\theta})$ (deg)	
	A_4 (a.u.)	A_4 (a.u.)		A_4 (a.u.)	$\Delta\theta'$ (deg)
ZnAl ₂ O ₄	(a) 36.35 (b) 36.53	36.12	0.0030	(a) 36.35 (b) 36.53	36.12
MgAl ₂ O ₄	1.956(a)	1.9530	0.0024	52.528(a)	52.521
ZnGa ₂ O ₄	1.970(b)	1.9662	0.0038	53.510(b)	53.507
Y ₃ Ga ₅ O ₁₂	2.015(b)	2.011	0.0040	53.844(b)	53.841
Y ₃ Al ₅ O ₁₂	2.019(b)	2.015	0.0040	54.175(b)	54.173
Be ₃ Al ₂ Si ₆ O ₁₈ ^a	2.020(a)	2.017	0.0030	57.344(a)	57.351
KAl(MoO ₄)	2.051(a)	2.049	0.0020	53.601(a)	53.600
RbSc(MoO ₄)	2.062(a)	2.0597	0.0033	55.909(a)	55.911
KSc(MoO ₄)	2.066(a)	2.063	0.0030	55.826(a)	55.829
RbIn(MoO ₄)	2.074(a)	2.070	0.0040	56.030(a)	56.040
Al ₂ O ₃	1.9534(b)	1.9489	0.0045	55.070(b)	55.067
LiNbO ₃	2.0405(b)	2.0359	0.0046	54.960(b)	54.960
LiTaO ₃	2.0382(a)	2.0355	0.0027	55.205(a)	55.203
Li ₂ O ₃	2.0640(b)	2.0616	0.0024	56.227(b)	56.228

^a Be₃Al₂Si₆O₁₈, the Trees correction $\alpha = 70 \text{ cm}^{-1}$ is also employing in the calculation.

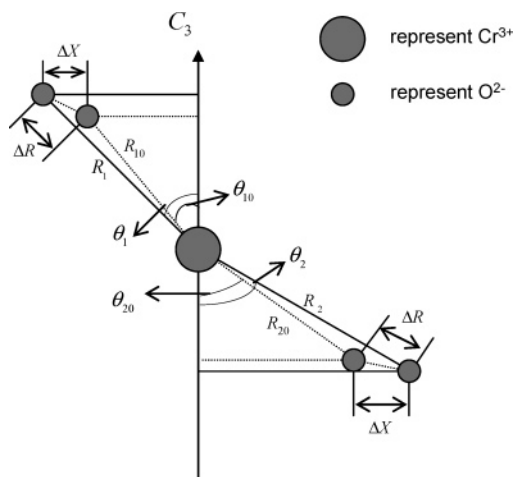


Figure 2. New model is used to describe the local structure of octahedral Cr^{3+} centers in oxide crystals with C_{3v} symmetry. R_{10} , R_{20} , θ_{10} , and θ_{20} are the structure parameters of the host crystals; R_1 , R_2 , θ_1 , and θ_2 are the impurity structure parameters. ΔR and ΔX denote the structure distortion.

2. Local Lattice Structures of the Octahedral $(\text{CrO}_6)^{9-}$ Clusters for Cr^{3+} Ion Doping in Oxide Crystals with C_{3v} Site Symmetry. Al₂O₃, LiIO₃, LiTaO₃, and LiNbO₃ have the same point symmetry C_{3v} . When Cr^{3+} ions are doped in oxide crystals, the Cr^{3+} ion will replace the host ions (Al³⁺, Li⁺, Ta⁵⁺, or Nb⁵⁺). The Cr^{3+} ion is surrounded by six oxygen ions which form an octahedron with a distortion along one of the C_3 axes. Similarly, the ligand field parameters may be written as

$$B_{20} = (3/2)[G_2(p_1)(3 \cos^2 \theta_1 - 1) + G_2(p_2)(3 \cos^2 \theta_2 - 1)]$$

$$B_{40} = (3/8)[G_4(p_1)(35 \cos^4 \theta_1 - 30 \cos^2 \theta_1 + 3) + G_4(p_2)(35 \cos^4 \theta_2 - 30 \cos^2 \theta_2 + 3)]$$

$$B_{43}^c = (3\sqrt{35}/4)[G_4(p_1) \cos \theta_1 \sin^3 \theta_1 + G_4(p_2) \cos \theta_2 \sin^3 \theta_2] \quad (12)$$

where $G_2(p_i)$ and $G_4(p_i)$ are expressed as

$$G_2(p_i) = -qeG^2(p_i) \\ G_4(p_i) = -qeG^4(p_i) \quad (13)$$

$$G^k(p_i) = \int_0^{R_{pi}} R_{3d}^{-2}(r) r^2 \frac{r^k}{R_{pi}^{k+1}} dr + \int_{R_{pi}}^{\infty} R_{3d}^{-2}(r) r^2 \frac{R_{pi}^k}{r^{k+1}} dr \quad (14)$$

p_1 and p_2 represent the ligand ions in the up and down three-edge-pyramids in oxide crystals and θ_1 and θ_2 represent the corresponding angles between metal–ligand bonds and the C_3 axis. Since the bond lengths of two three-edge-pyramids in oxide crystals are not the same, we may predict that

$$G_2(p_1) \neq G_2(p_2) \\ G_4(p_1) \neq G_4(p_2) \quad (15)$$

Similarly, $G_2(P_i)$ and $G_4(P_i)$ can be written as

$$G_2(P_i) = \frac{A_2}{R_{Pi}^3}, \quad G_4(P_i) = \frac{A_4}{R_{Pi}^5} \quad (16)$$

where the definitions of the A_2 and A_4 are the same as the above, in order to explain the trigonal distortion of impurity structure with C_{3v} symmetry reasonably, a new model is proposed, as shown in Figure 2. So the local structure parameters R_1 , R_2 , θ_1 , and θ_2 for Cr^{3+} replacing the host ions in octahedral $(\text{CrO}_6)^{9-}$ complexes can be expressed as a function of the ΔR and ΔX

$$R_1 = R_{10} + \Delta R, \quad R_2 = R_{20} + \Delta R \\ \theta_1 = \arcsin\left(\frac{R_{10} \sin(\theta_{10}) + \Delta X}{R_1}\right) \\ \theta_2 = \arcsin\left(\frac{R_{20} \sin(\theta_{20}) + \Delta X}{R_2}\right) \quad (17)$$

where R_0 and θ_0 denote the M–O (M = Al, Li, Nb, and Ta) bond length and the angle between M–O bond and the C_3 axis, respectively, and the values are listed in Table 5 [see refs 18 and 48–50]. As for the electrostatic parameters B and C , ζ and the orbit reduction factor k are also listed in Table 2. Using those parameters, the zero-field splitting parameter D , EPR g factors $g_{||}$ and g_{\perp} , and optical spectra as a function of ΔR and ΔX are calculated by diagonalizing the complete energy matrix, and the results are listed in Tables 6–9.

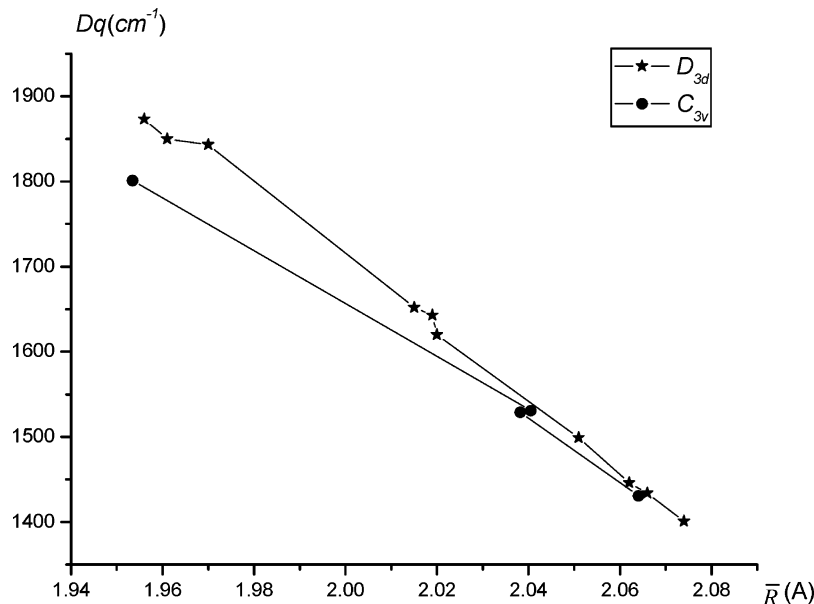


Figure 3. Theoretical values of D_q for $(\text{CrO}_6)^{9-}$ clusters plotted against the corresponding the average values \bar{R} of Cr–O bond length in oxide crystals with C_{3v} or D_{3d} symmetry.

From Tables 3, 4, 6, 7, 9, and 10, one can see that, when Cr^{3+} ion doping in a variety of oxide crystals with D_{3d} or C_{3v} site symmetry, the experimental findings of the zero-field splitting parameters, D , EPR g factors, $g_{||}$ and g_{\perp} , and optical spectra can be satisfactorily explained by corresponding distortion parameters, respectively. Moreover, it is indicated that the sign of the zero-field splitting D are consistent with that of the Δg . Correspondingly, the local structure parameters can also be determined, which are listed in Tables 1 and 8, respectively. According to Tables 1 and 8, the function of D_q vs \bar{R} is shown in Figure 3. It is shown that the average values of \bar{R} of Cr–O bond length decrease with the crystal field strength D_q rising except for the influence of the temperature in oxide crystals with C_{3v} or D_{3d} symmetry, which is consistent with the universal relation $D_q \propto 1/R^n$ ($n > 4$). It is further indicated that the calculated values of the Cr–O bond length for Cr^{3+} ion doping in a variety of oxide crystals with D_{3d} or C_{3v} site symmetry are reasonable.

From Tables 1, 8 and 11, we can see that the bond length of the octahedral $(\text{CrO}_6)^{9-}$ clusters and the angles between the M–O bond and C_3 axis are variational irregularly. However, although the local lattice structures around the M (M = Al^{3+} , Ga^{3+} , Li^+ , Sc^{3+} , etc.) ions in host crystals are obviously different, the local lattice structures of the octahedral $(\text{CrO}_6)^{9-}$ cluster in a variety of oxide crystals doped with Cr^{3+} ions are similar and fluctuant in the vicinity of that of the Cr_2O_3 . This may be ascribed to the fact that there is the similarly octahedral $(\text{CrO}_6)^{9-}$ clusters in a variety of oxide crystals doped with Cr^{3+} and the Cr_2O_3 crystal.

Moreover, from Table 11, both A_4 values derived from two different environments (Cr_2O_3 and $\text{MgO}:\text{Cr}^{3+}$) are applied to determine the local lattice structure of the octahedral $(\text{CrO}_6)^{9-}$ cluster, and the results show that the influences of the assumption A_4 on the precision of the structure parameters is very small and may be neglected. Furthermore, because the octahedral $(\text{CrO}_6)^{9-}$ cluster in the Cr_2O_3 crystal approaches the ideal $(\text{CrO}_6)^{9-}$ cluster, we suggest that the value of A_4 obtained from the Cr_2O_3 crystal should be employed in this calculation. In order to clarify the assumption in detail, careful experimental and theoretical investigations will be required to study a series of crystals in the future.

IV. Conclusions

Local lattice structures of Cr^{3+} complexes have been investigated on the basis of the complete energy matrix by studying the EPR and optical spectra simultaneously. The calculated results show that, although the local lattice structures around the M (M = Al^{3+} , Ga^{3+} , Li^+ , Sc^{3+} , etc.) ions in host crystals are obviously different, the local lattice structures of the octahedral $(\text{CrO}_6)^{9-}$ cluster in a variety of oxide crystals doped with Cr^{3+} ions fluctuate in the vicinity of that of the Cr_2O_3 . Moreover, the relation between crystal field strength D_q and the average values \bar{R} of Cr–O bond length derived from the calculated values is consistent with the universal relation $D_q \propto 1/R^n$ ($n > 4$), which further verifies that our results are reasonable.

Acknowledgment. This project was supported by the National Natural Science Foundation of China (Nos. 10774103 and 10374068) and the Doctoral Education fund of Education Ministry of China (No. 20050610011).

References and Notes

- Powell, M. J. D.; Gabriel, J. R.; Johnston, D. F. *Phys. Rev. Lett.* **1960**, 5, 145.
- Jain, V. K.; Lehmann, G. *Phys. Status Solidi B* **1990**, 159, 495.
- Watanabe, G. *Progr. Theor. Phys. (Kyoto)* **1957**, 18, 405.
- Gabriel, J. R.; Johnston, D. F.; Powell, M. J. D. *Proc. R. Soc. A* **1961**, 264, 503.
- Newman, D. J.; Ng, B. K. C. *Crystal field handbook*; Cambridge University Press: New York, 2000.
- Newman, D. J.; Urban, W. *Adv. Phys.* **1975**, 24, 793.
- Zheng, W. C.; Wu, S. Y.; Gong, M.; Zi, J. *Phys. Rev. B* **2002**, 66, 245206.
- Wu, S. Y.; Zheng, W. C. *Phys. Rev. B* **2002**, 65, 224107.
- Ma, D. P.; Zhang, J. P. *Phys. Rev. B* **2003**, 68, 054111.
- Kuang, X. Y.; Morgenstern-Badarau, I.; Rodriguez, M. C. *Phys. Rev. B* **1993**, 48, 6676.
- Kuang, X. Y. Ph.D. Thesis; Université de Paris-sud: Paris, 1994; p 14.
- Kahn, O. *Molecular Magnetism*; VCH Publishers, Inc.: New York, 1993; p 31.
- Abragam, A.; Bleany, B. *Electron Paramagnetic Resonance of Transition Ions*; Oxford University Press: London, 1970.
- Van Vleck, J. H. *J. Chem. Phys.* **1932**, 1, 208.
- Zhao, M. G.; Xu, J. A.; Bai, G. R.; Xie, H. S. *Phys. Rev. B* **1983**, 27, 1516.

- (16) Groh, D. J.; Pandey, R.; Recio, J. M. *Phys. Rev. B* **1994**, *50*, 14860.
- (17) Fairbank, W. M., Jr.; Klauminzer, G. K. *Phys. Rev. B* **1973**, *7*, 500.
- (18) McClure, D. S. *J. Chem. Phys.* **1962**, *38*, 2289.
- (19) Jørgensen, C. K. *Absorption spectra and chemical bonding in complexes*; Pergamon Press: London, 1962; p 290.
- (20) Bravo, D.; López, F. *J. Phys.: Condens. Matter.* **1992**, *4*, 10335.
- (21) Euler, F.; Bruce, J. A. *Acta Crystallogr.* **1965**, *19*, 971.
- (22) García-Lastra, J. M.; Aramburu, J. A. A.; Barriuso, M. T.; Moreno, M. *Phys. Rev. B* **2006**, *74*, 115118.
- (23) Klevtsova, R. F.; Klevtsov, P. V. *Kristallografiya* **1970**, *15*, 953.
- (24) Jain, V. K.; Lehmann, G. *Solid State Commun.* **1989**, *71*, 523.
- (25) Efremov, V. A.; Trunov, V. K.; Velikodnyi, Yu. A. *Kristallografiya* **1972**, *17*, 1135.
- (26) Wood, D. L.; Imbusch, G. F.; Macfarlane, R. M.; Kisliuk, P.; Larkin, D. M. *J. Chem. Phys.* **1968**, *48*, 5255.
- (27) Kahan, H. M.; Macfarlane, R. M. *J. Chem. Phys.* **1971**, *54*, 5197.
- (28) Wood, D. L.; Ferguson, J.; Knox, K.; Dillon, J. F., Jr. *J. Chem. Phys.* **1963**, *39*, 890.
- (29) Wood, D. J. *J. Chem. Phys.* **1965**, *42*, 3404.
- (30) Hermanowicz, K.; Maczka, M.; Dereń, P. J.; Hanuza, J.; Strek, W.; Drulis, H. *J. Lumin.* **2001**, *92*, 151.
- (31) Hermanowicz, K.; Hanuza, J.; Maczka, M.; Dereń, P. J.; Mugeński, E.; Drulis, H.; Sokolska, I.; Sokolnicki, J. *J. Phys.: Condens. Matter* **2001**, *13*, 5807.
- (32) McClure, D. S. *J. Chem. Phys.* **1962**, *36*, 2757.
- (33) Fairbank, W. M.; Klauminzer, G. K.; Schawlow, A. L. *Phys. Rev. B* **1975**, *11*, 60.
- (34) Macfarlane, Peter. I.; Holliday, Keith.; Nicholls, John. F. H.; Henderson, Brian. *J. Phys.: Condens. Matter* **1995**, *7*, 9643.
- (35) Ryba-Romanowski, W.; Golab, S.; Pisarski, W. A.; Dominiak-Dzik, G.; Palatnikov, M. N.; Sidorov, N. V.; Kalinnikov, V. T. *Appl. Phys. Lett.* **1997**, *70*, 2505.
- (36) Karthe, W. *Phys. Status Solidi B* **1977**, *81*, 323.
- (37) Belyaev, M. L.; Grechushnikov, B. N.; Dobrzhanskii, G. F.; et al. *Kristallografiya* **1977**, *22*, 650.
- (38) Tang, H. G.; Li, Y. K.; Miao, M. H.; Hang, Y. *Acta Opt. Sin.* **1986**, *6*, 155.
- (39) Struve, B.; Huber, G. *Appl. Phys. B* **1985**, *36*, 195.
- (40) Chen, Q. H.; Du, M. L. *J. Synth. Cryst.* **1989**, *18*, 130.
- (41) Wood, D. L.; Burke, W. E.; Van Uitert, L. G. *J. Chem. Phys.* **1969**, *51*, 1966.
- (42) Burns, G.; Geiss, E. A.; Jenkins, B. A.; Nathan, M. I. *Phys. Rev. B* **1965**, *139*, A1687.
- (43) Bai, X. M.; Zeng, L. W. *Phys. Rev. B* **1989**, *39*, 10.
- (44) Hermanowicz, K. *J. Alloys Compd.* **2002**, *341*, 179.
- (45) Zapart, M. B.; Zapart, W.; Zvyagin, A. I. *Bull. Acad. Pol. Sci. Ser. Sci. Phys. Astron.* **1980**, *28*, 35.
- (46) Zapart, M. B.; Zapart, W.; Stankowski, J. *Physica B* **1982**, *114*, 201.
- (47) Zapart, M. B.; Zapart, W.; Zvyagin, A. I. *Phys. Status Solidi A* **1984**, *82*, 67.
- (48) Chang, Y. M.; Yeom, T. H.; Yeung, Y. Y.; Rudowicz, C. *J. Phys.: Condens. Matter* **1993**, *5*, 6221.
- (49) Loyo-Menoyo, M.; Keeble, D. J.; Furukawa, Y.; Kitamura, K. *J. Appl. Phys.* **2005**, *97*, 123905.
- (50) Bouer, J. L.; Van Bolhuis, F.; Hazecamp, R. O.; Vos, A. *Acta Crystallogr.* **1966**, *21*, 841.
- (51) Nelson, H. M.; Larson, D. B.; Gardner, J. H. *J. Chem. Phys.* **1967**, *47*, 1994.
- (52) Drickamer, H. G.; et al. In *Solid State Physics*; Seitz, F., Turnbull, D., Eds.; Academic Press: New York, 1966; Vol. 19, p 135.
- (53) Malovichko, G.; Grachev, V.; Kokanyan, E.; Schirmer, O. *Phys. Rev. B* **1999**, *59*, 9113.
- (54) Karthe, W.; Kühmstedt, R. *Phys. Status Solidi B* **1974**, *63*, K5.